

Analysis of GPS Measurement in West-Java, Indonesia

Bambang SETYDJI*, Ichiro MURATA**, Joenil KAHAR***
S. SUPARKA****, Torao TANAKA*

*Research Center for Earthquake Prediction, DPRI, Kyoto University

**Earthquake Research Institute, University of Tokyo

***Dept. of Geodetic Engineering, ITB, Indonesia

****Indonesian Institute of Sciences

Synopsis

GPS Measurements for geodynamics study in West-Java, Indonesia, have been done several times, since 1992 by a cooperating group between Japan and Indonesia. For these measurements, 14 pillars have been settled to cover, for the first time, two geological structures, the Cimandiri and Lembang fault zones. These phenomena are assumed as one of the compensation of subduction process of Indo-Australian plate beneath the Eurasian plate in the south of Java Island, which has a velocity of 71 mm/yr at 20° azimuth relative to the Eurasian plate (NUVEL-1).

The December 1996 campaign gave a result with an rms error error between 0.4 and 3.5 mm, when one coordinate at ITB1 was kept fixed. The N-S components give rms error around 1.5 times better than the E-W and the height component, as expected, give three times larger than the horizontal components.

Comparing to previous campaigns, the 1996 campaign shows a trend of deformation vectors which are in agreement to the global model of plate tectonics. The northern part of the Cimandiri fault zone moved to the northeast direction, relative to ITB1 Station, which is laid in the southern part. The calculated strain from GPS result also shows that there is a compression process within the area in NE-SW direction

Keywords: GPS, deformation, strain, West-Java,

1. Introduction

The area of this study is the western part of Java Island in Indonesia (Fig. 1). This island is a part of the forearc island which is one of the compensation of the subduction process of the Indo-Australian plate beneath the Eurasian plate. The velocity of the Indo-Australian plate relative to the Eurasian plate from the NUVEL-1A vector is $71 \pm 2 \text{ mm a}^{-1}$ at $020 \pm 3^\circ$ azimuth. The subduction zone can be divided into two parts, the first one is a normal subduction which elongates from the Banda Sea through the Sunda Strait and forms Timor through and Java trench. The second part is an oblique subduction in the west of Sumatra Island which elongates to the Andaman Sea. The zone of increasing obliquity is in the southwest of Sunda Strait, about 500 km from the studied area.

There are two geological phenomena, the Cimandiri fault and the Lembang fault, which are assumed also as a compensation of the subduction process. Previous geological study shows that the Cimandiri fault is a sinistral slip fault, the northern part is moved in the southwest direction relative to the southern part. This fault is also suggested as the prolongation of the Pelabuhan Ratu fault, which happens at the sea floor of the accretionary prism zone of the subduction. These fault extends from the Pelabuhan Ratu gulf area to an area around Sukabumi. Meanwhile, the Lembang fault is laid about 8 km in the north of Bandung City, the capital of West Java province, and extends in the west-east direction. There is no clear geological evidence which shows that the Lembang fault is a part of the Cimandiri fault.

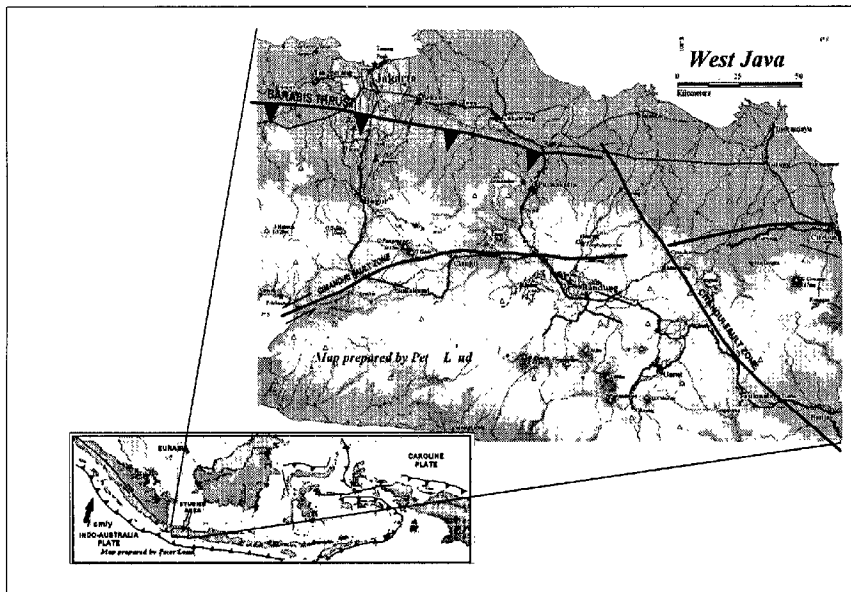


Figure. 1 Simplified tectonic setting of the studied area.

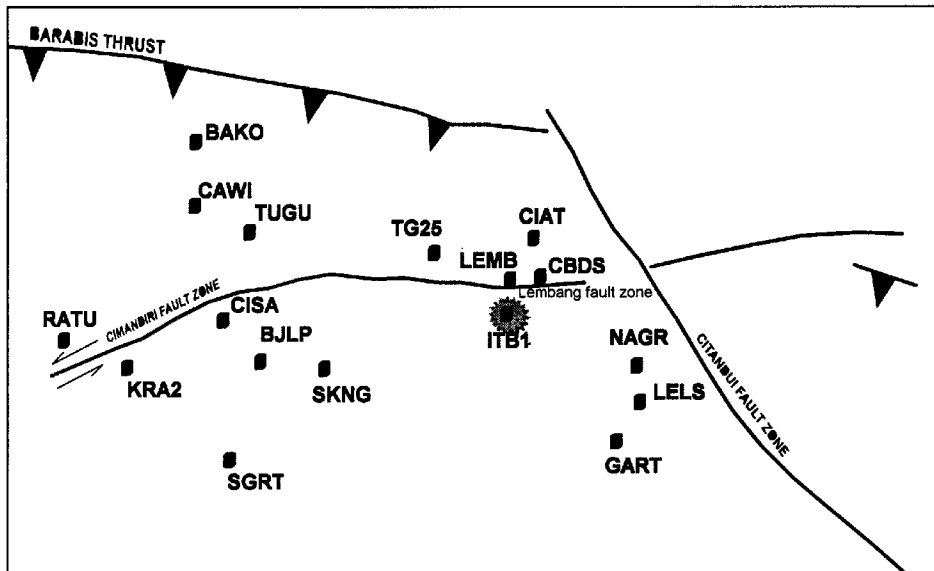


Figure. 2 Distribution of GPS Stations. Cimandiri fault is covered by western network, and Lembang fault is covered by eastern network

This study tries to examine the faults behavior by using another approach, the geodetic (geometric) approach. This approach will quantify the phenomena by mean of the displacement vectors, and their derived stress-strain setting. It can be done by determining the coordinates of some selected points several times and finding the displacement vectors from the difference of coordinates between each measurement. The GPS technology, which has the capability to measure a long range distance in a high precision level, was used to determine these coordinates.

For the purpose of this deformation study in West-Java area, Disaster Prevention Research Institute (DPRI) of Kyoto University in compliment with some Indonesian institutions has done some GPS campaigns since 1991 to 1996. The Indonesian counterparts are The Department of Geodesy - Institut Teknologi Bandung (ITB), and the Research and Development Center for Geotechnology - the Indonesian Institute for Sciences. (cf. Monbusho Project Report, 1995)

2. GPS Surveys

In totally, 17 stations were used in creating this Geodynamic GPS network (Fig. 2). 14 Stations, which can be separated into two sub-networks, have been built in the survey area (Tanaka *et al.*, 1994). The western network, which includes 8 points are mainly used for examining the Cimandiri fault behavior. Meanwhile the other 6 points in the eastern network were used for examining the Lembang Fault behavior. Other three points which were included into the network are the zero order National GPS Network point of Indonesia at the Indonesian Agency for Surveys and Mapping (Ind: *BAKOsurtanal*), the **ITB1** point at the top of the Post-Graduate faculty building of the Institut Teknologi Bandung, and the gravity calibration network (**GB03**) point near the Ciater hot spring resort. The first two points are being the reference point for GPS Processing.

The 1996 campaign involves one Ashtech Z-XII3 receivers and three Topcon Receivers of Kyoto-University. It occupied four stations; the ITB1 as the fix station, the NAGR, CBDS, and TUGU Points. The measurement were done at day time, from 10:00 to 16:00 local time (UTC+7). The recording interval was 30 second. The meteorological parameters i.e. temperature, air pressure and humidity, were recorded every 30 minutes at TUGU point.

3. Data Processing and Results

All the campaigns were re-processed using a same program and its configuration, and this paper will briefly explains the result of the December 1996 campaign only.

The (beat) carrier phase mode data of GPS observables are used for the postprocessing. The GPS data were processed using the Bernese V 4.0 Postprocessing Software for PC-DOS. The precise ephemerides information, which was used for

determining the precise orbits, was downloaded from one of the IGS FTP site.

These precise ephemerides files were used to produce satellite clock files by fitting the satellite clock information within intervals of 12 hours by low degree polynomials (in these case, we used the degree of $q = 2$). The resulted satellite clock files were used to compute satellite clock corrections for each observation epoch. Even the correction were based only on the pseudorange data, the corrected clocks were applied both to the pseudorange and phase data.

Then, the clock corrected phase data were used to create the dual-frequency single difference data or, in the other word, to create a baseline observation. The baselines were such pre-defined to make a possibility of calculating the coordinates network-wise, not only baseline-wise. It means that the normal equations of daily observations can be combined to perform a network solution. Before the phase processing step, these single-difference data were screened by a pre-processing algorithm to detect and repair the cycle slips.

In the phase processing, the *Quasi Ionospheric Free (QIF)* linear combination were used for resolving the ambiguities session-wise using L1 & L2. Then, the normal equation (NEQ) files were made on L3 by introducing the L1 & L2 ambiguities and kept all stations free. All the NEQ files then were combined to get the network solution over the network. The tropospheric zenith delay parameters were estimated every one hour of observation. (Rothacher and Mervart., 1996) These parameters were calculated using relative mode, which kept fixed at ITB1 point.

This December 1996 campaign gave the rms error below 1 (one) mm for horizontal components, and maximum 3.5 mm for vertical component (Table 1). These results came from combined solutions of three days measurements.

Table 1. Coordinates and rms error error of TUGU, CBDS, and NAGR points. The calculation were done by fixing the ITB1 Coordinates

| No | Stations | Latitude (° ' ") | Longitude (° ' ") | Height (m) |
|----|---------------|---------------------|----------------------|---------------|
| 2 | ITB1 | - 6 53 17.0590 | 107 36 32.5700 | 813.3970 |
| | rms error (m) | 0.0000 | 0.0000 | 0.0000 |
| 3 | NAGR | - 7 01 45.9891 | 107 54 5.2502 | 850.9812 |
| | rms error (m) | 0.0004 | 0.0008 | 0.0035 |
| 8 | CBDS | - 6 49 29.0598 | 107 41 11.4244 | 1279.4099 |
| | rms error (m) | 0.0004 | 0.0006 | 0.0031 |
| 15 | TUGU | - 6 42 10.4065 | 106 58 17.8672 | 1122.4144 |
| | rms error (m) | 0.0004 | 0.0008 | 0.0032 |

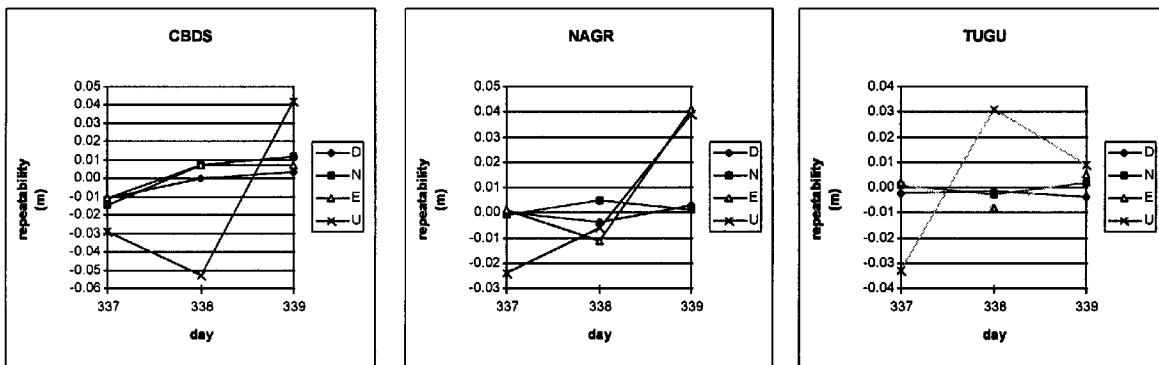


Figure. 3 Repeatabilities of December 1996 Campaign result. These three baselines were fixed at ITB1 Point.

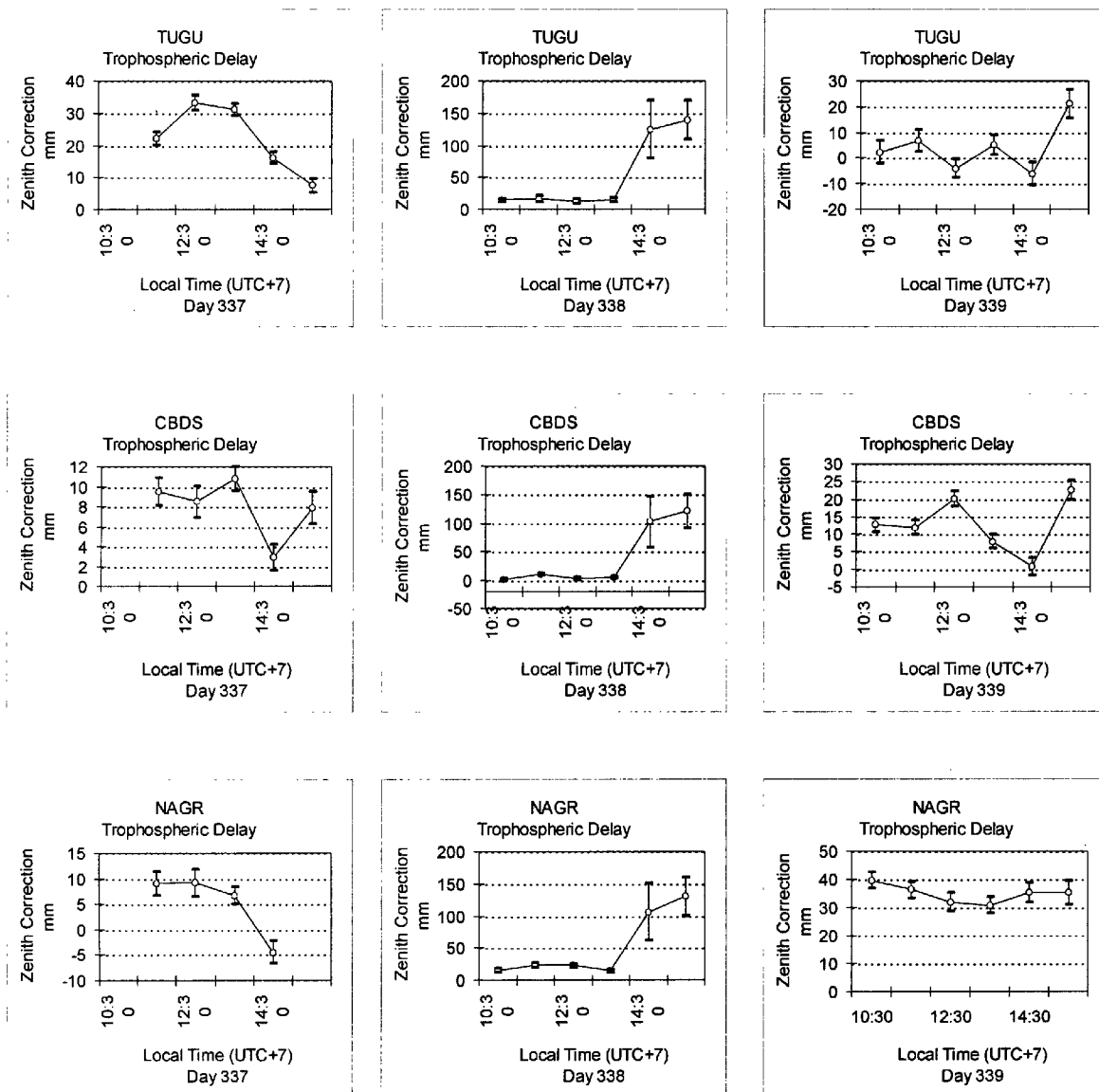


Figure. 4 Zenith correction of TUGU, CBDS, and NAGR points. Note that there was a heavy ice-rain on the day of 338, between 14:00 to 16:00 around ITB1 point

The daily repeatabilities for horizontal component are in the range of 2 (two) cm except for NAGR at the day of 338, when the east component made a high variation. Meanwhile the vertical component is in the range of 10 cm. The baselines repeatabilities are in the same range to the horizontal component. It seems that the high vertical variation did not influence the baselines length effectively. These repeatabilities are shown in Figure 3.

Table 2. Displacement rates of GPS Points

| No. | Station | Displacement rate (m/year) | | | notes |
|-----|---------|----------------------------|---------|---------|-------|
| | | N | E | U | |
| 1 | BAKO | 0.0008 | 0.0091 | 0.0946 | ** |
| 2 | ITB1 | 0.0000 | 0.0000 | 0.0000 | |
| 3 | NAGR | 0.0017 | 0.0049 | 0.0013 | *** |
| 4 | LELS | | | | N/A |
| 5 | GART | -0.0044 | 0.0070 | 0.0318 | * |
| 6 | TG25 | 0.0017 | 0.0045 | -0.0392 | * |
| 7 | LEMB | 0.0004 | 0.0055 | 0.0434 | * |
| 8 | CBDS | -0.0011 | 0.0012 | -0.0602 | *** |
| 9 | SKNG | 0.0060 | -0.0029 | 0.1338 | * |
| 10 | SGRT | 0.0087 | 0.0206 | -0.1444 | * |
| 11 | BJLP | 0.0066 | 0.0054 | -0.0626 | * |
| 12 | RATU | 0.0024 | 0.0277 | 0.0778 | ** |
| 13 | CISA | 0.0029 | 0.0150 | 0.1711 | ** |
| 14 | CIAW | 0.0074 | 0.0017 | -0.1019 | * |
| 15 | TUGU | 0.0039 | -0.0031 | 0.0056 | * |
| 16 | CIAT | 0.0018 | -0.0159 | 0.0416 | * |
| 17 | KRA2 | 0.0081 | -0.0010 | 0.1716 | ** |

* 93 - 96, ** 93 - 94, *** 94 - 96

The tropospheric zenith delay estimation gave the result in the range of 40 mm except on the day of 338. There was a large jump up to 15 cm at the end of the session, and suggested as an effect of heavy ice-rain around the fixed ITB1 point. Figure 4 shows the tropospheric zenith delay for TUGU, CBDS, and NAGR point.

4. Deformation Analysis

The deformation analysis is done by calculating the strain components from the displacement rates of the GPS stations. This displacement rates were derived from the 5 GPS campaigns. The resulted rates are shown in Table 2. The results are the combination of all the 5 campaigns. The displacement rate vectors are shown in Fig. 5.

If the northern part of the eastern network movement can be represented by the CIAT point and the southern part by the GART point, the displacement of northern part is about 6.7 cm/year in west direction relative to southern part.

The western network shows a more complicated displacements. There are two movement trends in this network. The TUGU, SKNG, and KRA2 seem to move northwest direction, meanwhile the rest of the point trend to the northeast direction. Sub-network BAKO-CAWI-TUGU shows a clock-wise rotation.

The strain components were calculated using simple rigid body deformation model which used by Caspary (1984). This model derived from the 3-dimensional coordinates transformation concept which involves 7 transformation parameters. 6 (six) parameters represent the translations in X, Y and Z direction and rotations around X, Y, and Z. The seventh parameter, the scaling factor, represents the deformation, in term of strain parameters, of the

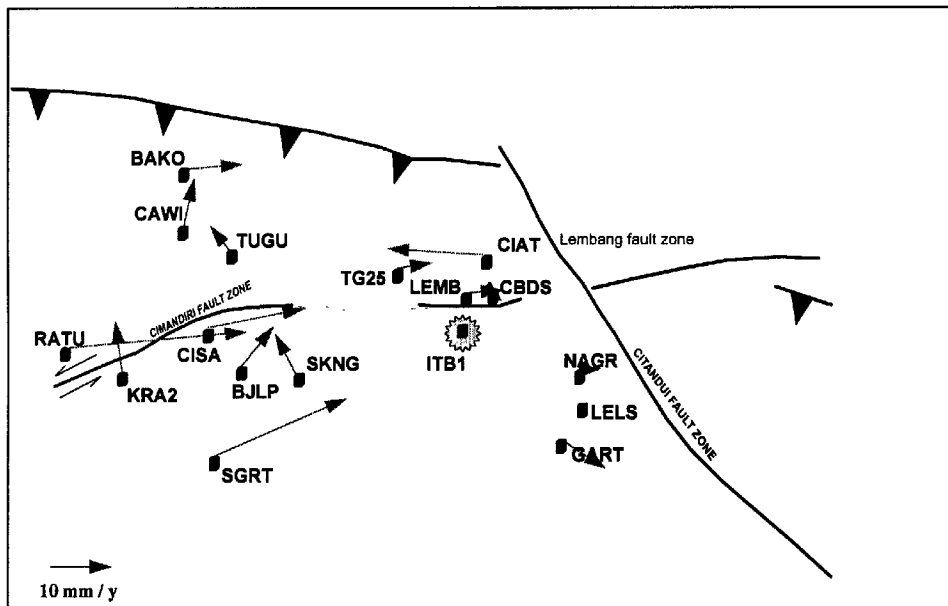


Figure 5. Illustration of Vector of Displacement rate of the GPS stations. Also see Table 2.

bounded area. Due to the lower accuracy of the vertical components, the transformation parameters are reduced into 4 parameters. The Z axis translation and two rotation around X and Y axes are omitted.

Strain computations were done in three different groups. The first group involves only western network (Cimandiri fault), the second one the eastern network (Lembang fault), and third one all the network (Fig. 6.a and 6.b). Table 3 shows the calculated translation and strain components.

Fig 6.a shows the strain parameters for two case, which are associated with the strain for Cimandiri fault and Lembang fault separately. The maximum principal strains shows the same tendency of the compressional strain in the NE-SW direction. But the minimum principal strains are different. There exist compressional strain in Cimandiri fault and tensional strain in Lembang fault.

The calculation which involves all the points gives a smaller compressional strain than the separate calculations, but in the same NE-SW direction. The other principal strain is a tensional strain like in the case of lembang fault, but much smaller than it.

5. Conclusion

The calculated strain parameters seems to be in agreement to the global model of plate tectonics. The maximum compressional strain direction in Cimandiri and Lembang faults are in the same trend to the NUVEL-1 model of the subduction direction of Indo-Australian plate of N20°E .

This is also in agreement to the local geological evidence. Qualitatively, the strain setting around Cimandiri fault zone might be capable to produce a left lateral strike slip fault.

The network has been extended to an active volcano at Garut, in the southern of Bandung. It is recommended to extent the network more to the eastern part to covers another fault zone, the Citandui fault zone.

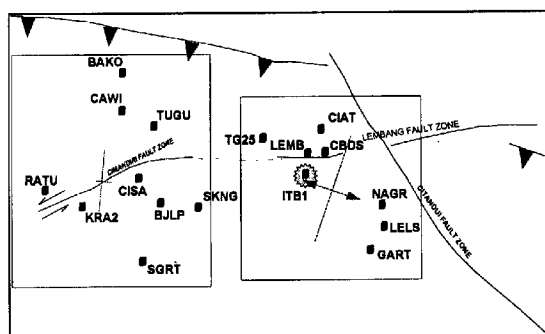
References

Tanaka, T. 1995: Monbuscho International Scientific Research Program (1994), *Disaster Prevention Research Institute*, Kyoto University, Kyoto.

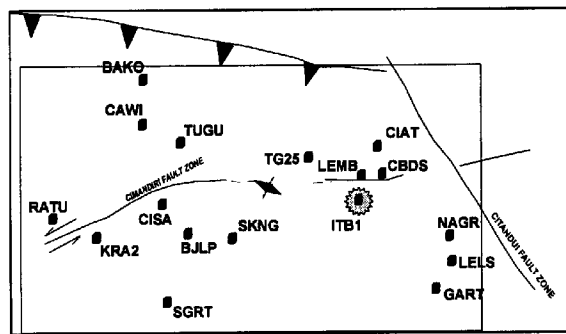
Tanaka, T., J. Kahar, F. Kimata, I. Murata, S. Okubo, Kamtono, W. Kuntjoro, K. Nakamura, Ponimin M.

Table 3. Displacement and strain parameters. t_x , t_y , and ω are the translation in X and Y, and the rotation of the region respectively. ϵ_1 and ϵ_2 are the principal strain parameters, and θ is the angle of ϵ_1 from X axis. Negative strain means a compressional strain

| Deformation Components | Cimandiri Fault | Lembang fault | All points |
|------------------------------|-----------------|---------------|--------------|
| t_x (mm) | 7.5 | 5.1 | 4.1 |
| t_y (mm) | 4.8 | -1.0 | 2.7 |
| ω (") | 0.0087 | 0.0528 | 0.0089 |
| ϵ_1 (μ strain) | -0.0600 | 0.1995 | 0.0415 |
| ϵ_2 (μ strain) | -0.2460 | -0.4085 | -0.1535 |
| θ (° ' ") | 8 26 17.2763 | 21 20 0.1879 | 37 16 9.8081 |



6.a



6.b

Fig 6.a. Calculating the strain by separating the area into two networks. b. The strain are calculated with involves all the stations

S., K. Prijatna, B. Setyadji, S. Miura, K. Villanueva, E. Hendrayana, A. Soewandito, K. Sarah, Augustine E.P., J. Rais, K. Hirahara, S. Suparka. (1994): Monitoring of Crustal Movements by GPS and Gravity Change around Volcanoes and Active Fault System, *Japan-Indonesia Joint Research on Natural Hazard Prediction and Mitigation*, Disaster Prevention Research Institute, Kyoto University, Kyoto.

Rothacher, M., and Leos Mervart, ed. (1996): Bernese GPS Software Version 4.0. *Astronomical Institute*, University of Berne, Bern.

Caspary, W.F. (1987): Concept of Network and Deformation Analysis, *Monograph 1, School of Surveying*. The University of New South Wales, Kensington.

要 旨

インドネシアのジャワ島西部では、1992年以来日本の共同研究として数回のGPS観測を行ってきた。ジャワ島の南でインド・オーストラリアプレートがユーラシアプレート下へ沈み込むために生じる運動を反映しているものと解されているCimandiriおよびLembang両断層の現在の運動を調べるため14点からなる観測網を設置した。1996年12月の観測における平均二乗誤差は0.4~3.5mmとなり、南北成分は東西成分に比べ1.5倍、また上下成分は約3倍悪い。以前の観測と比較した結果は、インド・オーストラリアプレートの沈み込みによる変形を調和している。Cimandiri断層の北側は北東方向への動きを示唆しており、南側は圧縮の傾向をしめしている。

キーワード:GPS 地殻変動 ひずみ 西ジャワ